Electron transit time and reliable mobility measurements from thick film hydroxyquinoline-based organic light-emitting diode

Tse, S. C.; Fong, H. H.; So, S. K.

Published in:
Journal of Applied Physics

DOI:
10.1063/1.1589175

Published: 01/08/2003

Document Version:
Publisher's PDF, also known as Version of record

Electron transit time and reliable mobility measurements from thick film hydroxyquinoline-based organic light-emitting diode

S. C. Tse, H. H. Fong, and S. K. So[a)]
Department of Physics, Hong Kong Baptist University, Kowloon Tong, Hong Kong, China

(Received 13 February 2003; accepted 12 May 2003)

The time delay (τ_d) in the transient electroluminescence (EL) signal of a bilayer organic light-emitting diode with a structure of indium-tin oxide /*N*,*N*′-diphenyl-*N*,*N*′-bis(3-methylphenyl)-(1,1′-biphenyl)-4,4′-diamine /tris(8-hydroxyquinoline) aluminum (Alq_3)/Al has been measured and analyzed as a function of the thickness (D) of the Alq_3 layer. For a thin layer of Alq_3 ($D<180$ nm), it is found that τ_d is affected by both the charging effect and carrier transit time through the Alq_3 layer. For a thicker layer of Alq_3 ($D>200$ nm), τ_d approaches the intrinsic electron transit time through Alq_3. Electron mobility of Alq_3 can be evaluated for the thick-film devices and the results are in excellent agreement with independent time-of-flight measurements. The application of transient EL in mobility measurement for C540-doped Alq_3 is discussed. © *2003 American Institute of Physics.* [DOI: 10.1063/1.1589175]

I. INTRODUCTION

Organic light-emitting diodes (OLEDs) are making steady advances in display technology since the pioneer work of Tang and VanSlyke.[1] While there have been numerous attempts to improve device performances, considerable efforts are now being made to understand the fundamental materials and device physics relating to OLEDs. One of the interesting issues in OLED operation is the transient electroluminescence (EL) response of an OLED after a rectangular voltage pulse excitation. A time delay is found to occur between the application of the voltage pulse and the onset of EL signal.[2–4] Normally, the device for transient EL has a bilayer organic structure of indium-tin oxide (ITO)/hole transporter layer (HTL)/electron transporter layer (ETL)/cathode. In some cases, tris(8-hydroxyquinoline) aluminum (Alq_3) is adopted as the electron transporter as well as the light-emitting layer.[2,5,6] Under such a circumstance, the EL time delay is often attributed to the transit time of electrons through the Alq_3 layer.[2,4] The transit time of holes through the HTL is generally much shorter as hole mobilities are roughly 2–3 orders of magnitude higher than electron mobility in Alq_3.[7,8] Similar models have also been applied to polymeric light-emitting diodes (LEDs) with reasonable performance.[9–11]

Recently, this simple view has been put into challenge, especially in Alq_3-based bilayer OLEDs.[12,13] Instead of solely attributing the delay time to the electron transit time, the delay time is thought to have a more complex dependence on the carrier dynamics. The elementary processes involved include charge carrier injection, carrier transit, buildup of space charges, excitons formation at the interface, and radiative recombination. Thus, it seems to be nontrivial to separately identify the effect of each process on the EL delay time.

To address the interpretation of delay time in the transient EL signal, we have performed a systematic thickness dependence study on the delay time in transient EL using Alq_3-based bilayer OLEDs. We show that for Alq_3 with a thickness less than 180 nm, the electron mobility deduced from the delay time underestimates the intrinsic electron mobility. On the other hand, for Alq_3 with a thickness greater than 200 nm, the EL time delay is dominated by the transit time of the electron through the Alq_3 layer, and the electron mobility deduced is thickness independent. To verify this, we measured the intrinsic mobility in thick-film OLEDs and the electron mobility in a bulk film (~ 9 μm) of Alq_3 using the optical time-of-flight (TOF) technique. TOF transients indicate that electron transport in Alq_3 is essentially nondispersive in the absence of oxygen, and has a Poole–Frenkel (PF) dependence. The mobility results from transient EL and TOF are in excellent agreement with each other. The performance of transient EL in mobility determination lends confidence to the determination of electron mobility in more complex materials system. To demonstrate its applicability, transient EL is used to determine the electron mobilities of Alq_3 doped with C540. C540 is an important dopant for enhancing the EL signal in Alq_3-based device via Förster-type energy transfer.[14] So, it would be interesting to see how the electron mobility of Alq_3 is altered upon doping.

II. EXPERIMENT

The organic materials used in this study are Alq_3, TPD, and C540, and their chemical structures are shown in Fig. 1.[15] Alq_3 was obtained from H.W. Sands and was purified once by train zone sublimation prior to thin-film coating. The other materials were used as received without further purification. For transient EL measurements, the device had a basic structure ITO/TPD(60 nm)/Alq_3(D nm)/Al where D varied from 60–250 nm. The emitting area of the device was about 4 mm^2. All film thicknesses were determined *in situ* by a calibrated quartz-crystal sensor and *ex situ* by a profilome-

a)Author to whom correspondence should be addressed; electronic mail: skso@hkbu.edu.hk

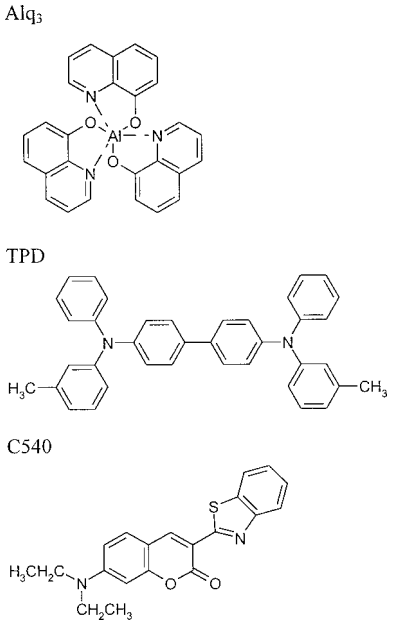

FIG. 1. Chemical structures of organic molecules.

ter. For electron mobility measurements in pristine Alq_3, the time delay of the onset of EL was measured from which the apparent electron mobility was deduced. For electron mobility measurements of doped Alq_3, the Alq_3 layer was altered so that only 20 nm of Alq_3 next to TPD remained undoped while the rest was doped with C540 at 10% concentration by volume. The total thickness of the doped Alq_3 layer was 200 nm. The structures for the undoped and doped devices are shown in Fig. 2(a). In all cases, samples were prepared in a high-vacuum evaporator with a base pressure of about 1×10^{-6} Torr. The coating rate was 1 Å/s for undoped Alq_3 unless stated otherwise. For doped Alq_3, the coating rate was 10 Å/s for the host and 1 Å/s for the dopant. After coating, the transient EL samples were immediately encapsulated in an atmosphere of dry nitrogen. In TOF measurements, the sample had a structure of ITO/Alq_3(8.73 μm)/Al. The coating rate was 10 Å/s for Alq_3. Immediately after coating, the TOF sample was loaded into a cryostat which was evacuated to a pressure of 1×10^{-3} Torr.

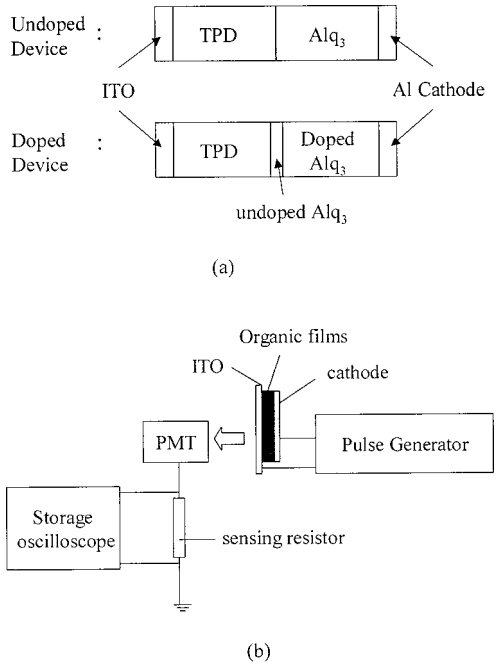

FIG. 2. (a) OLED device structures, and (b) the experimental setup for transient EL measurements.

The experimental setup for transient EL measurements is shown in Fig. 2(b). During measurement, a rectangular voltage pulse (amplitude 10–80 V, pulse duration 1–20 μs) was applied to an OLED using a pulse generator (HP Model 241B). The time-resolved EL from the OLED was measured by placing a miniature photomultiplier tube (PMT) (Hammamatsu Model 5783-02) directly on the top of the OLED. The output photocurrent from the PMT was sourced into a sensing resistor from which the transient EL signal can be displayed on a storage oscilloscope (Agilent Model 54622A). To avoid artifacts from instrumentation, an inorganic LED was used as a test sample which exhibited a negligible time delay for the onset of EL. The details for the experimental setup for TOF measurements have been described elsewhere.[8] Briefly, a nitrogen pulsed laser (Laser Science, $\lambda=337.1$ nm, pulse width 4 ns) was used to generate photocarriers. The laser beam was directed from the ITO side to create electron–hole pairs near the ITO/Alq_3 interface. A dc power supply was used to provide the bias voltage for electron detection. A current sensing resistor R in series with the sample was used to detect the electron photocurrent. A digital oscilloscope (HP54600B) was used to measure the voltage across R.

III. RESULTS AND DISCUSSIONS

A typical transient EL signal for a device with a structure ITO/TPD(60 nm)/Alq_3($D=220$ nm)/Al is shown in the top panel of Fig. 3. The transient EL signal can be characterized by a time delay (τ_d) in the onset of EL, followed by a gradual rise in the EL intensity before reaching the saturated EL intensity, an EL overshoot right after the pulse is off, and the final decay of the EL signal. The bottom panel shows a few more transient EL signals with increasing applied voltage amplitudes from Figs. 3(a)–3(e). From the top panel of Fig. 3, $\tau_d=0.3$ μs. With increasing applied voltages, τ_d is observed to become smaller. In this study, we will be primarily concerned with the interpretation of τ_d and its relation to the electron transit time in Alq_3-based bilayer OLEDs.

Following the detailed analysis of the previous studies in this area of research, we will attribute the delay time τ_d primarily to the sum of the interfacial charging time and the transit time of electrons through the Alq_3 layer.[12,13,16,17] The interfacial charging time can be understood as the time required to accumulate space charges at the TPD/Alq_3 interface to facilitate electron injection from the Al cathode. The voltage drop across the TPD layer is negligible.[18] Bearing this in mind, one can compute the *apparent* electron mobility from τ_d according to the well-known relation:

$$\mu_e=\frac{D}{\tau_d\cdot F}, \tag{1}$$

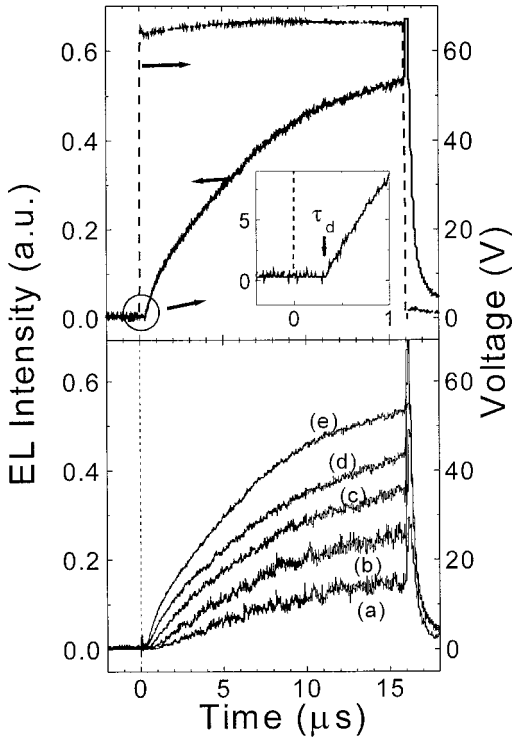

FIG. 3. Top panel: A typical transient EL signal for an OLED with a device structure ITO/TPD(60 nm)/Alq(220 nm)/Al; bottom panel: A set of transient EL signals for the same device under different applied fields. From (a)–(e), the field strengths are 2.04, 2.23, 2.50, 2.77, and 3.04 MV cm^{-1}, respectively.

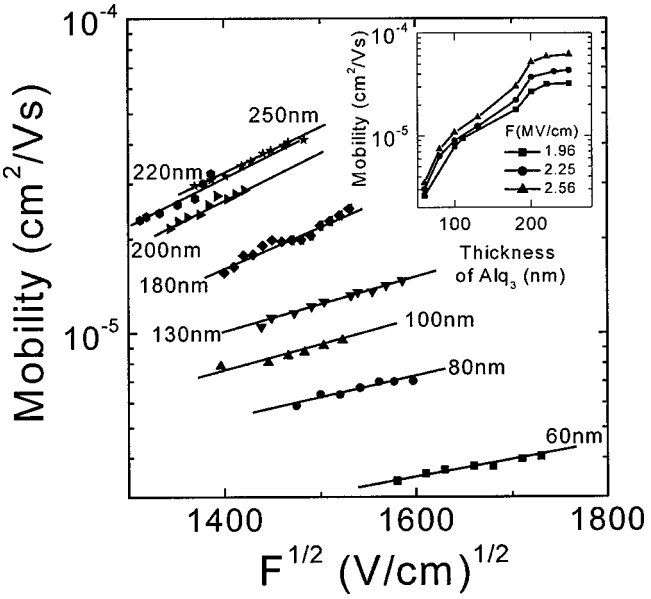

FIG. 4. Apparent electron mobility, μ_e, vs the square root of the applied field for different Alq_3 thicknesses D. The solid lines are the best fits to the data sets. The inset shows the dependence of μ_e on D under different field strengths.

where D is the thickness of the Alq_3 layer and F is the electric field inside Alq_3. If we make the additional assumptions: (1) the built-in potential in the interface is small compared to the applied voltage, and (2) the electric field is uniform throughout the Alq_3 layer, then the applied field $F \approx V/D$ for an external applied voltage pulse of amplitude V. Using Eq. (1) and the aforementioned assumptions, the apparent electron mobility of Alq_3 in the bilayer OLEDs can be computed.

Values of μ_e computed from Eq. (1) are shown in Fig. 4 in a PF plot where $\log \mu_e$ is plotted against $F^{0.5}$ for different values of D (60–250 nm). All data can be fitted by the phenomenological PF equation:

$$\mu_e = \mu_0 \exp(\beta\sqrt{F}), \tag{2}$$

where β is the PF slope. Several observations can be made. First, for small Alq_3 thickness D (e.g., $D=60$ nm), μ_e has a relatively weak field dependence and has a value between $3-4\times10^{-6}$ $cm^2\,V^{-1}\,s^{-1}$ in the field range of 2.3–3 MV cm^{-1}[$1500<F^{0.5}<1750$ $(V\,cm^{-1})^{0.5}$]. The apparent mobility μ_e has a very similar trend and values as those reported recently under similar assumptions.[12] As $D \approx 60$ nm is the optimum Alq_3 thickness for efficient OLED operation,[19] most of the reported transient EL experiments reported so far were focused in this thickness range.[2,3,12] Second, with increasing D, μ_e increases monotonically until $D > 200$ nm. (See also Fig. 4, inset.) For example, for $F = 2.3$ MV cm^{-1} [$F^{0.5}\approx1500$ $(V\,cm^{-1})^{0.5}$], μ_e increases roughly ten times from 3×10^{-6} to 4×10^{-5} $cm^2\,V^{-1}\,s^{-1}$ as D increases from 60 to 250 nm. However, when $D > 200$ nm, μ_e becomes insensitive to thickness changes. Third, the PF plot acquires a steeper slope, i.e., a large β and hence a stronger field dependence in μ_e as D increases. (See also Fig. 5.) However, the value of β tends to saturate as $D>200$ nm, and reaches a saturation value of 4.0×10^{-3} $(cm\,V^{-1})^{0.5}$. Summarizing the observations from Figs. 4 and 5, we can deduce that for small thickness D, the computed μ_e deviates substantially from the intrinsic electron mobility since it is unphysical that the mobility should be thickness dependent. Furthermore, the insensitivity of μ_e and β to thickness for $D>200$ nm is an indication that the computed μ_e is approaching the true values of the intrinsic electron mobility in Alq_3.

To verify the reliability of electron mobility determination in EL samples with thick Alq_3 layers, we performed

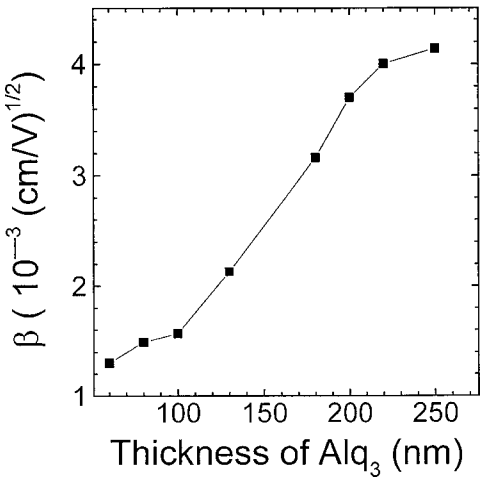

FIG. 5. The dependence of the PF slope β on Alq_3 thicknesses.

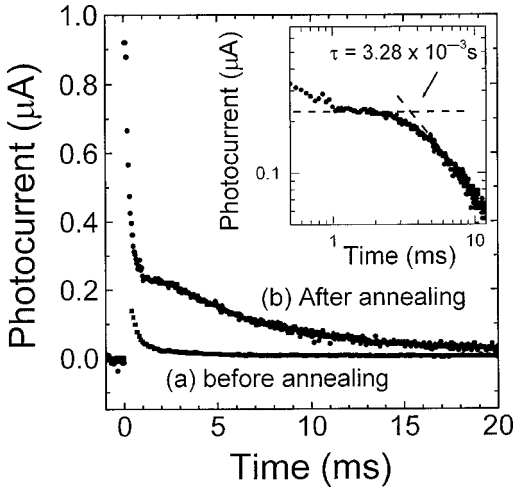

FIG. 6. TOF photocurrent transient for Alq_3 (a) before and (b) after annealing. The inset is a log–log plot showing clearly the electron transit time.

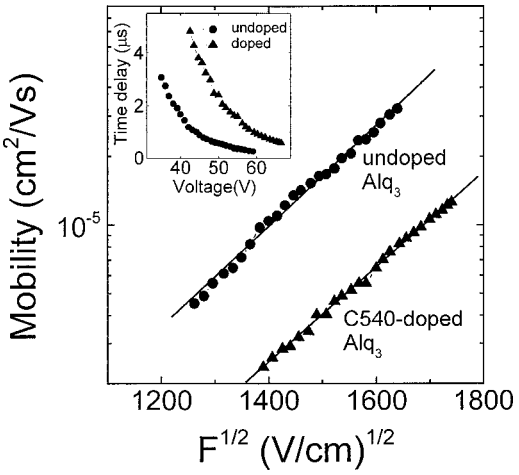

FIG. 8. Electron mobilities of undoped and C540-doped Alq_3. The inset indicates the corresponding EL time delays.

direct TOF measurements on bulk films of Alq_3. Figure 6 is a typical example of electron photocurrent transient recorded for bulk Alq_3 film (8.7 μm). When a freshly prepared TOF sample is exposed to air, the TOF photocurrent is highly dispersive and it is difficult to determine the carrier transit time [Fig. 6(a)]. Previously, we showed that the dispersive behavior can be associated with oxygen traps or moisture inside Alq_3.[20,21] By annealing the TOF sample to 370 K for 12 h in a vacuum and cooling the sample to room temperature, a nondispersive TOF transient with a clear carrier transit time can be observed. Following this procedure, the intrinsic electron mobility can be determined [Fig. 6, inset]. The results from TOF are summarized in Fig. 7 (squares). It can be observed that the electron mobility follows the PF form quite well. The electron mobility spans the range from 0.1 to 1×10^{-6} $cm^2\,V^{-1}\,s^{-1}$ while the electric field F varies from $0.4-0.9\ MV\,cm^{-1}[600<F^{1/2}<950\ (V\,cm^{-1})^{1/2}]$.

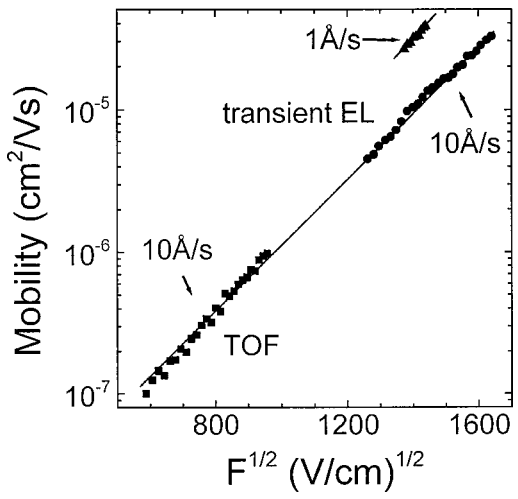

FIG. 7. Electron mobility of Alq_3 obtained from transient EL measurements (circles) for a device structure of ITO/TPD(60 nm)/Alq(220 nm)/Al, and electron mobility of Alq_3 determined by TOF measurement (squares) for a thick film (8.73 μm) of Alq_3. The same coating rate of 10 Å/s was used for Alq_3 in both cases. The solid line is the best line fit for both sets of data. Triangles are transient EL data with an Alq_3 coating rate of 1 Å/s.

Higher field mobility measurement was not possible from TOF as an exceedingly large biased voltage must be applied on the sample. In Fig. 7, we also show the electron mobility determined from transient EL measurements (circles) using a bilayer OLED with $D=220$ nm. For this particular OLED, a coating rate of 10 Å/s was used for Alq_3 (same rate as the TOF sample) as the coating rate is known to affect the electron mobility in Alq_3.[6] (Mobility from transient EL for a device with an identical structure, but with a coating rate of 1 Å/s is also shown.) The transient EL data follows the usual PF form, but the mobility is now smaller than the case with a 1 Å/s coating rate. The difference can be attributed to the presence of more disorder in the present case. The field range covered is in the high-field region where F varies from $1.5-2.7\ MV\,cm^{-1}[1350<F^{0.5}<1650(V\,cm^{-1})^{0.5}]$. Low-field measurements were not possible from transient EL as the signal-to-noise ratio became quite small. Although the two sets of data do not overlap with each other, they practically form linear extrapolation of each other as indicated by the solid line in Fig. 7. Hence, the data all together in Fig. 7 is a direct verification of the reliability in electron mobility determination from thick-film samples by transient EL.

The validity of Eq. (1) in determining intrinsic mobility from transient EL deserves further comments. For a thick-film sample, the listed assumptions become valid. First, the delay time τ_d is affected both by interfacial charging and carrier transit time. But, as D increases, the interfacial charging time remains unchanged while the transit time begins to dominate. So τ_d can be interpreted as the carrier transit time in Eq. (1) for thick-film samples. Similar observations have been reported previously from transient EL in light-emitting Langmuir–Blodgett films.[3] Next, the built-in potential is known to have a value of about 1–2 V.[5,12] For thick-film sample, the typical applied voltage is at least 30 V, and therefore, the built-in potential can be safely ignored in Eq. (1).

To demonstrate the applicability of the transient EL technique in mobility determination, we have performed transient EL measurements on C540-doped Alq_3 sample. The device structure has already been shown in Fig. 2(a). In Fig. 8, inset, the delay time (τ_d) in transient EL is plotted versus

the applied voltage for both doped and undoped devices. After doping, there is a substantial increase in τ_d. The increase in τ_d can be entirely attributed to the increase in electron transit time through the doped-Alq_3 layer rather than the interfacial charging time because the same HTL/ETL interface is present in both the doped and undoped devices. From the increase in time delay, and neglecting the voltage drop in the thin layer (20 nm) of Alq_3 next to the TPD layer, the electron mobility in C540-doped Alq_3 can be evaluated, and the results are shown in Fig. 8. The electron mobility in the doped sample exhibits a rigid downward shift in the PF plot with respect to the undoped case. The general reduction in electron mobility can be understood as the effect of carrier trapping or scattering by the C540 dopant. An examination of the energy levels of C540 suggests the former factor plays a key role as the lowest unoccupied molecular orbital of C540 is about 0.2 eV below that of Alq_3.[22]

Compared to other low work function cathode systems (e.g., MgAg alloy or LiF/Al), an Alq_3-based OLED with an Al cathode tends to have a large operating voltage. In an attempt to reduce the driving voltage, we inserted a thin (0.5 nm) layer of LiF between Alq_3 and Al. As expected, there is a significant reduction in driving voltage. Concurrently, an apparent increase in the electron mobility can be deduced from transient EL experiments. The origin of this enhancement is not clear and deserves further investigations. It has been reported that Li atoms are liberated after the deposition of Al on LiF/Alq_3, and results in a Li-doped Alq_3 layer.[23] A similar observation has been observed for MgAg alloy on Alq_3 as Mg atoms diffuse into Alq_3 at about 360 K.[24] As the electron mobility of intrinsic Alq_3 is the main theme of this study, an Al cathode is a reasonable choice. Our TOF experimental results also independently support the choice of an Al cathode in transient EL experiments.

Although TOF experiments can, in principle, provide direct mobility measurements, transient EL does have its own benefits. Whereas TOF requires thick films of several microns for a well-defined flight distance, transient EL merely needs a film thickness of a fraction of a micron. Hence, there is a significant reduction in material consumption in the latter technique. Moreover, transient EL can yield high-field mobility whereas TOF can only yield low-field data. Further exploration of transient EL is underway.

IV. CONCLUSIONS

The electron mobility of Alq_3 has been measured by transient EL experiments using bilayer OLEDs. The device structure is ITO/TPD(60 nm)/Alq_3(D nm)/Al where D varies from 60–250 nm. The time delay (τ_d) for the onset of the EL signal can be observed. For sufficiently thick (>200 nm) Alq_3, τ_d is dominated by the transit time of electrons across the Alq_3 layer. The electron mobility extracted from τ_d is independent of the thickness of the Alq_3 layer and in excellent agreement with optical TOF measurements. The electron mobility follows the PF form closely in all cases. For a thin (<180 nm) Alq_3 layer, the delay time τ_d is affected by the growth of interfacial charging and the transit time, and it is not reliable to use the delay time to evaluate the electron mobility. Transient EL was also employed to measure the electron mobility of C540-doped Alq_3. A substantial reduction in electron mobility is attributed to trapping of carriers by the C540 dopant.

ACKNOWLEDGMENTS

Support of this research by the Research Committee of Hong Kong Baptist University under Grant No. FRG/00-01/II-14, and the Research Grant Council of Hong Kong under Grant No. HKBU/2063/00P are gratefully acknowledged.

[1] C. W. Tang and S. A. VanSlyke, Appl. Phys. Lett. **51**, 913 (1987).
[2] C. Hosokawa, H. Tokailin, H. Higashi, and T. Kusumoto, Appl. Phys. Lett. **60**, 1220 (1992).
[3] A. J. Pal, R. Osterbacka, K. M. Kallman, and H. Stubb, Appl. Phys. Lett. **71**, 228 (1997).
[4] Y. Kawabe and J. Abe, Appl. Phys. Lett. **81**, 493 (2002).
[5] W. Brütting, S. Berleb, and A. G. Mückel, Org. Electr. **2**, 1 (2001).
[6] B. J. Chen, W. Y. Lai, Z. Q. Gao, C. S. Lee, S. T. Lee, and W. A. Gambling, Appl. Phys. Lett. **75**, 4010 (1999).
[7] S. Heun and P. M. Borsenberger, Chem. Phys. **200**, 245 (1995).
[8] H. H. Fong, K. C. Lun, and S. K. So, Chem. Phys. Lett. **353**, 407 (2002).
[9] Y.-H. Tak, H. Vestweber, H. Bässler, A. Bleyer, R. Stockmann, and H. H. Hörhold, Chem. Phys. **212**, 471 (1996).
[10] V. Savvateev, A. Yakimov, and D. Davidov, Adv. Mater. (Weinheim, Ger.) **11**, 519 (1999).
[11] J. Wang, R. G. Sun, G. Yu, and A. J. Heeger, J. Appl. Phys. **91**, 2417 (2002).
[12] W. Brütting, H. Riel, T. Beierlein, and W. Riess, J. Appl. Phys. **89**, 1704 (2001).
[13] S. Barth, P. Müller, H. Riel, P. F. Seildler, W. Riess, H. Vestweber, and H. Bässler, J. Appl. Phys. **89**, 3711 (2001).
[14] C. W. Tang, S. A. VanSlyke, and C. H. Chen, J. Appl. Phys. **65**, 3610 (1989).
[15] The full name for TPD is N,N′-diphenyl-N,N′-bis(3-methylphenyl)-(1,1′-biphenyl)-4,4′diamine; C540 is Coumarin 540.
[16] B. Ruhstaller, S. A. Carter, S. Barth, H. Riel, W. Riess, and J. C. Scott, J. Appl. Phys. **89**, 4575 (2001).
[17] K. Book, H. Bässler, V. R. Nikitenko, and A. Elschner, Synth. Met. **111**, 263 (2000).
[18] M. Hiramoto, K. Koyama, K. Nakayama, and M. Yokoyama, Appl. Phys. Lett. **76**, 1336 (2000).
[19] S. K. So, W. K. Choi, L. M. Leung, and K. Neyts, Appl. Phys. Lett. **74**, 1939 (1999).
[20] G. G. Malliaras, Y. Shen, D. H. Dunlap, H. Murata, and Z. H. Kafafi, Appl. Phys. Lett. **79**, 2582 (2001).
[21] H. H. Fong, K. C. Lun, and S. K. So, Jpn. J. Appl. Phys., Part 2 **41**, L1122 (2002).
[22] K. Yamashita, J. Futenma, T. Mori, and T. Mizntani, Synth. Met. **111**, 87 (2000).
[23] G. Parthasarathy, C. Shen, A. Kahn, and S. R. Forrest, J. Appl. Phys. **89**, 4986 (2001).
[24] P. He, F. C. K. Au, Y. M. Wang, L. F. Cheng, C. S. Lee, and S. T. Lee, Appl. Phys. Lett. **76**, 1422 (2000).